

# Trading water for carbon: Sustained photosynthesis at the cost of increased water loss during high temperatures in a temperate forest

Anne Griebel<sup>1</sup>, Lauren T. Bennett<sup>2</sup>, Daniel Metzen<sup>1</sup>, Elise Pendall<sup>1</sup>, Patrick N.J. Lane<sup>3</sup>, and Stefan Arndt<sup>4</sup>

<sup>1</sup>Hawkesbury Institute for the Environment, Western Sydney University, Locked Bag 1797, Penrith, NSW 2570, Australia

<sup>2</sup>School of Ecosystem and Forest Sciences, The University of Melbourne, 4 Water St, Creswick, VIC 3363, Australia

<sup>3</sup>School of Ecosystem and Forest Sciences, The University of Melbourne, Parkville, VIC 3010, Australia

<sup>4</sup>School of Ecosystem and Forest Sciences, The University of Melbourne, 500 Yarra Boulevard, Richmond, VIC 3121, Australia

November 21, 2022

## Abstract

Forest carbon and water fluxes are often assumed to be coupled as a result of stomatal regulation during dry conditions. However, recent observations have indicated increased transpiration rates during isolated heat waves across a range of eucalypt species under experimental and natural conditions, with inconsistent effects on photosynthesis (ranging from an increase to a near total decline). To improve the empirical basis for understanding carbon and water fluxes in forests under hotter and drier climates, we measured the water use of dominant trees, and the ecosystem-scale carbon and water exchange in a mature temperate eucalypt forest over three summer seasons. The forest maintained photosynthesis within 16% of peak photosynthesis rates during all conditions, despite up to 70% reductions in canopy conductance during a 5-day heatwave. While carbon and water fluxes both decreased by 16% on exceptionally dry summer days, GPP was sustained at the cost of up to 74% increased water loss on the hottest days and during the heatwave. This led to ~40% variation in ecosystem water use efficiency over the three summers, and ~two-fold differences depending on the way water use efficiency is calculated. Furthermore, the forest became a net source of carbon following a 137% increase in ecosystem respiration during the heat wave, highlighting that the potential for temperate eucalypt forests to remain net carbon sinks under future climates will depend not only on their potential to maintain photosynthesis during higher temperatures, but also on responses of ecosystem respiration to changes in climate.

1 **Trading water for carbon: Sustained photosynthesis at the cost of increased water loss**  
2 **during high temperatures in a temperate forest**

3 **Anne Griebel<sup>1,2\*</sup>, Lauren T. Bennett<sup>3</sup>, Daniel Metzen<sup>1,4</sup>, Elise Pendall<sup>1</sup>, Patrick N.J. Lane<sup>4</sup>,**  
4 **Stefan K. Arndt<sup>2</sup>**

5 <sup>1</sup> Hawkesbury Institute for the Environment, Western Sydney University, Locked Bag 1797,  
6 Penrith, NSW 2570, Australia

7 <sup>2</sup> School of Ecosystem and Forest Sciences, The University of Melbourne, 500 Yarra Boulevard,  
8 Richmond, VIC 3121, Australia

9 <sup>3</sup> School of Ecosystem and Forest Sciences, The University of Melbourne, 4 Water St, Creswick,  
10 VIC 3363, Australia

11 <sup>4</sup> School of Ecosystem and Forest Sciences, The University of Melbourne, Parkville, VIC 3010,  
12 Australia

13 \*Corresponding author: Anne Griebel (a.griebel@westernsydney.edu.au)

14 **Key Points:**

- 15 • GPP of temperate eucalypts was sustained at the cost of increased water use during hot  
16 periods, but both fluxes decreased during dry periods.
- 17 • WUE estimates for the same period differed up to two-fold depending on the way it was  
18 calculated.
- 19 • Doubling of ecosystem respiration turned the forest from a net sink into a net source of  
20 carbon during a longer heatwave.

21 **Abstract**

22 Forest carbon and water fluxes are often assumed to be coupled as a result of stomatal regulation  
23 during dry conditions. However, recent observations have indicated increased transpiration rates  
24 during isolated heat waves across a range of eucalypt species under experimental and natural  
25 conditions, with inconsistent effects on photosynthesis (ranging from an increase to a near total  
26 decline). To improve the empirical basis for understanding carbon and water fluxes in forests under  
27 hotter and drier climates, we measured the water use of dominant trees, and the ecosystem-scale  
28 carbon and water exchange in a mature temperate eucalypt forest over three summer seasons. The  
29 forest maintained photosynthesis within 16% of peak photosynthesis rates during all conditions,  
30 despite up to 70% reductions in canopy conductance during a 5-day heatwave. While carbon and  
31 water fluxes both decreased by 16% on exceptionally dry summer days, GPP was sustained at the  
32 cost of up to 74% increased water loss on the hottest days and during the heatwave. This led to  
33 ~40% variation in ecosystem water use efficiency over the three summers, and ~two-fold  
34 differences depending on the way water use efficiency is calculated. Furthermore, the forest  
35 became a net source of carbon following a 137% increase in ecosystem respiration during the heat  
36 wave, highlighting that the potential for temperate eucalypt forests to remain net carbon sinks  
37 under future climates will depend not only on their potential to maintain photosynthesis during  
38 higher temperatures, but also on responses of ecosystem respiration to changes in climate.

39 **1 Introduction**

40 A hotter and drier future is likely for many of Australia's ecosystems. Australia's mean annual  
41 temperature has increased by 1 °C since 1910, temperature distributions have shifted towards  
42 higher average monthly maximum and minimum temperatures, and the duration, frequency and  
43 intensity of extreme heat events has increased (BOM 2016a). The years 2013-2015 were among  
44 the top 10 hottest years on record, including a number of significant heatwaves in southeast  
45 Australia (BOM 2013, 2014, 2015). In addition, southeastern Australia has become drier due to  
46 severe rainfall deficiencies since the year 2000 (BOM 2016b). This indicates increased potential  
47 for climate-induced stress in Australian ecosystems, given projections of warmer and drier  
48 conditions over much of the Australian continent in coming decades (IPCC 2013). This will likely  
49 result in more hot days and fewer cool days, in addition to more time spent in drought as winter  
50 and spring rainfall is predicted to decrease further (BOM 2016a).

51 Over 900 eucalypt species occur in a broad range of climates in Australia, some with relatively  
52 narrow distributions, which could make them vulnerable to a changing climate (Brouwers et al.,  
53 2013; Hughes et al., 1996; Jurskis, 2005), and especially to extreme climate events (Choat et al.,  
54 2012; Matusick et al., 2013; Mitchell et al., 2014a). Many eucalypt species close their stomata to  
55 prevent excessive water loss in response to dry conditions (Breshears et al., 2013; Eamus et al.,  
56 2008), which delays embolisms in the stem xylem (Choat et al., 2012; Tyree & Sperry, 1989) at  
57 the cost of decreases in photosynthesis and increases in the vulnerability of leaves to heat and light  
58 stress (McDowell et al., 2008; McDowell, 2011; Mitchell et al., 2014b; Thomas & Eamus, 1999;  
59 Whitehead & Beadle, 2004). Stomatal conductance varies with supply and demand for CO<sub>2</sub> by  
60 photosynthesis (intercellular CO<sub>2</sub> concentration), leaf irradiance and leaf temperature, as well as  
61 atmospheric vapor pressure deficit and leaf turgor (Ball et al., 1987; Cowan, 1978; Medlyn et al.,

2011; Tuzet et al., 2003). Hence, photosynthesis, transpiration and stomatal conductance are commonly assumed to be coupled; that is, photosynthesis and transpiration both decrease with increasing stomatal regulation under most environmental conditions (Farquhar & Sharkey, 1982; Leuning, 1995; Tuzet et al., 2003). However, isolated studies provide evidence of a decoupling of photosynthesis from stomatal conductance in some tree species during extreme heat stress (Ameye et al., 2012; De Kauwe et al., 2019; Drake et al., 2018; Urban et al., 2017). For example, photosynthesis decreased in seven eucalypt forests (De Kauwe et al., 2019) or was near zero in 1-year-old *E. parramattensis* saplings (Drake et al., 2018) as water loss increased under high temperatures. This indicates that latent cooling of leaves by transpiration might be an important mechanism to cope with extended heat stress (Drake et al., 2018), in turn affecting the plant's carbon assimilation rate per unit stomatal conductance as well as the plant's water use efficiency (WUE). Nonetheless, in other temperate forest types dominated by eucalypts, photosynthesis increased with transpiration during a single heat wave event (van Gorsel et al., 2016), highlighting the need for further studies of concurrent carbon and water fluxes across an extended range of weather conditions.

Individual studies of transpiration cooling under heat stress have largely focused on young plants (Ameye et al., 2012; Drake et al., 2018; Urban et al., 2017), whereas direct measures of stomatal conductance, carbon assimilation (GPP) and transpiration at the ecosystem level remain challenging. Canopy conductance ( $G_c$ , as an approximation of stomatal conductance) is commonly derived by inverting the Penman-Monteith equation using directly measured latent heat flux (LE; Monteith, 1965). WUE has been estimated as the sum of GPP over the sum of ET, but this does not account for the non-linear response of LE to vapor pressure deficit (VPD). Thus, alternative formulations of ecosystem-scale WUE as underlying WUE (Zhou et al., 2015, 2014), or as intrinsic

85 WUE (Beer et al., 2009; Lloyd et al., 2002; Schulze and Hall, 1982) have been suggested to more  
86 accurately understand the underlying physiological mechanisms.

87 Studies examining concurrent carbon and water fluxes under heat stress in natural mature eucalypt  
88 forests are limited to isolated heatwave events (De Kauwe et al., 2019; van Gorsel et al., 2016).  
89 Further, it remains unclear if eucalypts respond differently to multi-day heatwaves compared with  
90 individual hot days, and how such responses might be mediated by water availability. As this is  
91 currently neither well understood, nor integrated into process-based ecosystem models, it limits  
92 the potential to predict how future climates characterized by more frequent and intense heatwaves  
93 will influence the physiology, productivity, and distribution of temperate forest eucalypts. We  
94 combined three years of concurrent sap flow and eddy covariance summer measurements in a  
95 natural temperate eucalypt forest to examine the dynamics of photosynthesis and water use during  
96 the hottest days, the driest days, and a 5-day heatwave. We hypothesized that (i) photosynthesis  
97 and transpiration would both decrease on the driest days and both increase on the hottest days  
98 (assuming no water limitations); and (ii) a longer heatwave would result in decreased carbon  
99 uptake and increased water loss, as photosynthesis decreases, and evapotranspiration increases  
100 during continuous temperature stress (assuming no water limitations). Our results have globally  
101 relevant implications for understanding the trade-offs between photosynthesis and water use from  
102 terrestrial ecosystems during exceptionally hot or dry conditions, which remain yet to be  
103 incorporated into plant hydraulic and land surface models.

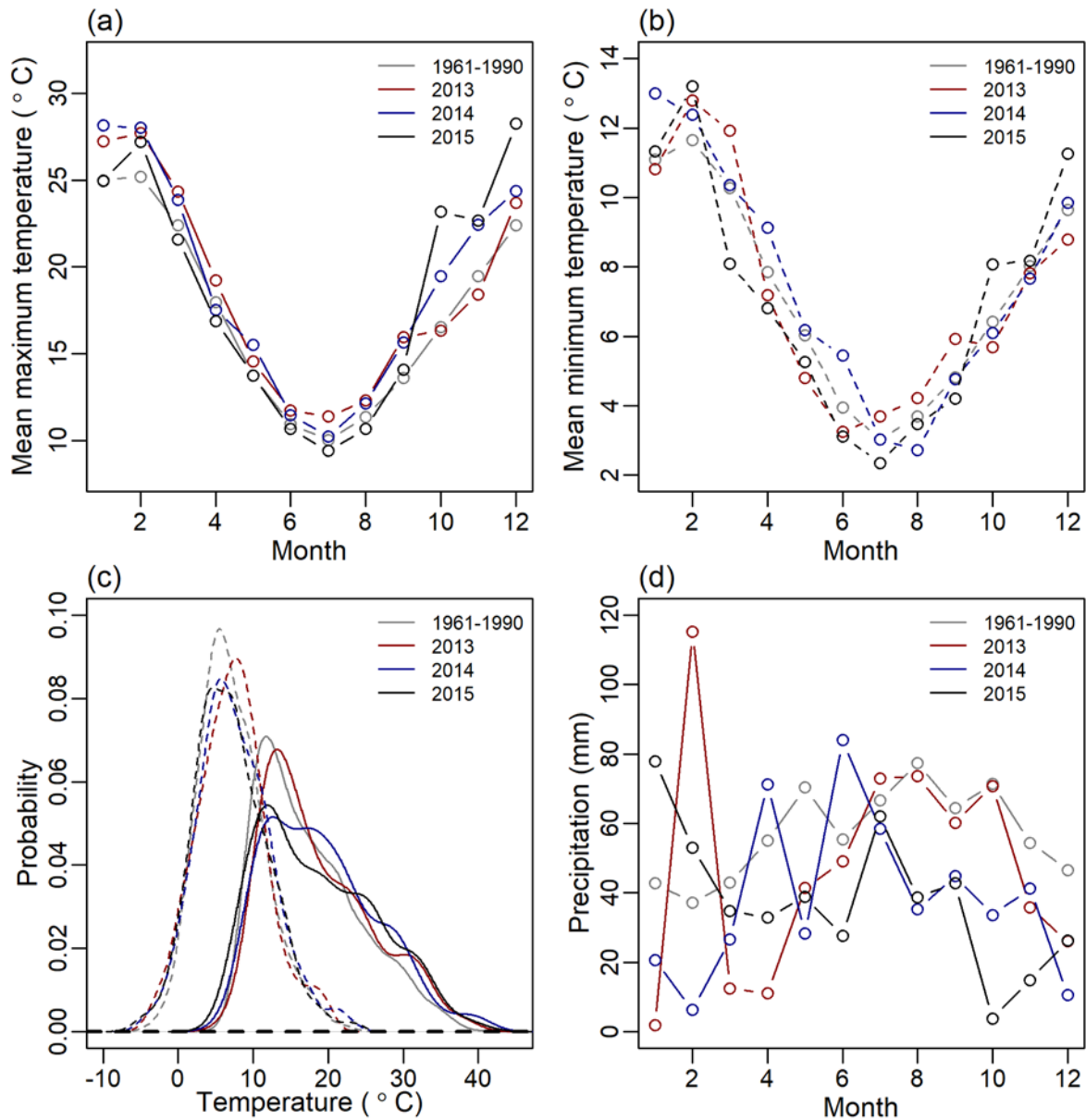
## 104 **2 Materials and Methods**

### 105 2.1 Study site and climate

106 We recorded tree water use and ecosystem carbon and water fluxes in a temperate mixed-species  
107 eucalypt forest (Wombat State Forest) in southeastern Australia from January 2013 to November  
108 2015. The study site is located near a ridge at 705 m elevation with gently sloping terrain to the  
109 southwest and northwest ( $< 8^\circ$ ; Griebel et al., 2016), approximately 100 km west of Melbourne,  
110 Australia, and is part of the TERN-SuperSite Network, TERN-OzFlux and FluxNet (AU-Wom),  
111 Sapfluxnet (AUS-WOM) and Dendroglobal network (AU-Wombat). Active forest management  
112 has been minimal since the late 1970s, with previous management practices including selective  
113 harvesting, low-intensity prescribed burning and firewood collection. The overstorey of this dry  
114 sclerophyll forest is dominated by three eucalypt species: *Eucalyptus obliqua* L'Hér (deep fibrous  
115 'stringybark'), *E. rubida* H. Deane and Maiden (smooth 'gum' bark), and *E. radiata* Sieber ex DC  
116 (short fibrous 'peppermint' bark; 70%, 21% and 9% of stand biomass, respectively; Griebel 2016),  
117 while the understory consists of sparse and patchy perennial grasses and the fern Austral bracken.  
118 The leaf area index (LAI, acknowledging that it includes leaves and woody biomass) was relatively  
119 stable in the first half of the study period (LAI  $\sim 1.7 \text{ m}^2 \text{ m}^{-2}$ ), and subsequently increased by  $\sim 20\%$   
120 by the end of the study period (Griebel et al., 2017).

121 The climate is cool temperate, with typically cool and wet winters, and warm summers. The closest  
122 weather station to the study site (Ballarat Aerodrome,  $\sim 20$  km distance) recorded a long-term  
123 average annual temperature of  $12.2^\circ\text{C}$  and an average annual rainfall of 690 mm (1908-2015).  
124 While the mean annual temperatures of the three study years were slightly below the long-term  
125 average ( $12.0^\circ\text{C}$  in 2013,  $11.8^\circ\text{C}$  in 2014 and  $10.8^\circ\text{C}$  in 2015), mean monthly maximum and  
126 minimum temperatures were generally greater than the World Meteorological Organization

127 (WMO) reference period (1961-1990) in spring and summer (baseline based on Ballarat  
128 Aerodrome data; Fig. 1a,b). Likewise, probability distributions of the mean monthly minimum and  
129 mean monthly maximum temperatures indicated a high likelihood for warmer temperatures during  
130 each study year (Fig. 1c). The annual rainfall totals were within 90 mm of the long-term average  
131 of 690 mm (780 mm in 2013, 672 mm in 2014 and 679 mm in 2015), but the 2014 and 2015  
132 monthly rainfall totals were consistently below the WMO reference totals in winter and spring  
133 (Fig. 1d).



134

135 **Figure 1.** Mean monthly maximum (a) and minimum (b) temperatures in spring (months 9 to 11)  
 136 and summer (months 1,2 and 12) were often higher during the three observation years than the  
 137 WMO reference period (1961-1990). This affected the likelihood of higher maximum  
 138 temperatures (solid lines, panel c) and to a lesser degree higher minimum temperatures (dashed  
 139 lines). Rainfall distribution (monthly rainfall totals, d) during the three years was erratic during  
 140 summer and autumn, but below average conditions in winter and spring in 2014 and 2015.

141 One of southeast Australia's most significant heatwaves (i.e. up to 12 °C higher than the 1961-  
142 1990 January mean maximum; BOM 2014) coincided with our study period in January 2014, and  
143 involved five consecutive days reaching ~35 °C and a peak vapor pressure deficit (VPD) of 5.4  
144 kPa at our study site. Thus, all references to heatwaves in this paper refer to this local heatwave  
145 ('HW', 13 to 17 January 2014), rather than the broader-scale 'Angry summer' of 2013 (van Gorsel  
146 et al., 2016), which affected much of southeastern Australia but was comparatively mild at our  
147 study site due to the >700 m elevation (i.e. isolated days with maximum temperatures in the low  
148 30s °C).

149 Since the 2014 heatwave was preceded by numerous rain events at the end of 2013 (i.e. was hot  
150 but well-watered), we also pooled the hottest and driest days throughout the summer months  
151 (December to February 2013-2015) for comparison with the 5-day heatwave. Here, the hottest  
152 days were those in the upper 90th percentile of maximum daily temperatures in summer (>30.7  
153 °C; 19 days), and the driest days were those in the lowest 10 percent of summer dryness as  
154 indicated by soil moisture sensors at 40 cm depth (<0.102 m<sup>3</sup> m<sup>-3</sup>; 23 days). The 19 hottest days  
155 excluded the heatwave from 13 to 17 January 2014 and did not overlap with any of the 23 driest  
156 days. Note that soil moisture sensors at greater depths (65 cm, 1m; see 'Climate variables and  
157 response functions') were installed too late to capture all summer months. In addition to the WMO  
158 1961-1990 baseline, we defined a local January baseline ('Base'; 59 unique days) as days in  
159 January 2013, 2014 and 2015 that excluded unusual weather conditions during part of the 'Angry  
160 summer' from 1 to 19 January 2013, the heatwave from 13 to 17 January 2014, as well as the  
161 hottest and driest 10% of days. The incoming solar radiation was comparable between the three  
162 groups (Table 1 and Fig. S1), and the soil moisture was comparable during the baseline, the hottest  
163 days and the heatwave. Thus, apart from the driest days (which were warm and dry), the four

164 groups primarily differed in their temperature range and associated atmospheric demand (which  
165 increased from the baseline to the driest days, the hottest days, and peaked during the heatwave;  
166 Table 1).

## 167 2.2 Sap flow measurements

168 Sap velocity ( $v_{\text{sap}}$ ) was monitored half-hourly from 1 January 2013 to 31 October 2015 in eleven  
169 trees: six *E. obliqua* (mean diameter at breast height, DBH = 41 cm, range 30.8 - 50.9 cm), and  
170 five *E. rubida* (mean DBH = 33.3 cm, range 22.8 - 46.7 cm). All trees were healthy and all canopies  
171 had access to direct sunlight. Crown class as identified by canopy position (Smith et al., 1997) was  
172 evenly distributed between species, with two intermediate and three sub-dominant trees per  
173 species, and one dominant *E. obliqua* (no dominant *E. rubida* were present). We utilized the heat  
174 pulse compensation method to monitor sap velocity (The HeatPulser, Edwards Industries, Taupo,  
175 NZ), and distributed four probes per tree with increasing implantation depth to cover the sap  
176 velocity gradient (mean sapwood depth: *E. rubida*  $1.95 \pm 0.42$  cm; *E. obliqua*  $1.92 \pm 0.38$  cm).  
177 Sap velocity was corrected for deviations from exact parallel spacing of the heater and the  
178 thermistor elements, and wounding size was determined for all probes at the end of the study  
179 period. In addition, tree cores were collected next to each probe to correct measured  $v_{\text{sap}}$  for the  
180 individual gas and water fractions of the sapwood of each instrumented tree (Edwards and  
181 Warwick 1984). Sap velocities were calculated for each probe and then averaged per tree. Each  
182 probe was analyzed for velocity drifts relative to the other three probes per tree, and affected probes  
183 were excluded from the analysis (2 probes in total). Data gaps through intermittent probe failures  
184 were filled with a hierarchical system to avoid an offset in the signal if either the fastest or slowest  
185 sensors were not working: 1. Gaps of individual probes were filled based on the highest fit of a  
186 regression between the probe that needed filling and the other three probes in the same tree (a

187 probe was only chosen when  $R^2 > 0.5$ ). If the fit with any probe of the same tree was below the  
188 threshold, then the best fit with a probe from all other trees was chosen to fill the gap. 2. The  $v_{sap}$   
189 means of each tree were gap-filled if there were periods with a data gap affecting all probes of a  
190 tree simultaneously (e.g. during a power outage, during data downloads or sensor repairs). Here,  
191 we correlated the means of all trees with each other and chose the tree with the best fit. The lowest  
192 correlation between two trees had a Pearson R of 0.85, so no minimum threshold had to be applied.

### 193 2.3 Eddy covariance measurements

194 We monitored ecosystem-scale carbon and water exchange from a flux tower adjacent to the trees  
195 that were monitored for  $v_{sap}$  dynamics. Fluxes were recorded at 30 m height with an open-path  
196  $CO_2/H_2O$  analyzer (LI-7500, LI-COR Biosciences, Lincoln, NE, USA) and a 3-D sonic  
197 anemometer (CSAT3, Campbell Scientific Inc., Logan, UT, USA), sampled at 10 Hz and averaged  
198 over 30 minute intervals. Flux data were processed with ‘OzFluxQC’ version 2.9.5  
199 (<https://github.com/OzFlux/OzFluxQC>), which included outlier removal through de-spiking, 2D  
200 co-ordinate rotations, WPL correction (Webb et al., 1980), conversion of virtual to sensible heat  
201 flux, and linear corrections for calibration anomalies and sensor drift (Griebel et al., 2017). We  
202 used the built-in neural network from OzFluxQC (SOLO; Isaac et al., 2017) for gap-filling of  
203 meteorological variables and fluxes. Data gaps of up to three hours were filled using linear  
204 interpolations, while longer gaps were filled with a descending preference of using alternative  
205 weather station data (Ballarat Aerodrome, ca. 20 km from study site), ACCESS model output from  
206 the Bureau of Meteorology, and BIOS2 model output, and lastly, using site-specific half-hourly  
207 averages of monthly climatology data (Isaac et al., 2017). We used 90-day intervals to gap-fill  
208 drivers and monthly intervals to gap-fill fluxes. Fluxes of carbon, water, and latent and sensible  
209 heat were gap-filled using incoming shortwave radiation, specific humidity deficit, and soil

210 temperature as independent variables. Year-specific friction velocity thresholds were determined  
211 with the change-point detection method using 1000 iterations following Barr et al. (2013), which  
212 were subsequently applied for partitioning of net ecosystem exchange (NEE) into gross primary  
213 productivity (GPP) and ecosystem respiration (ER). Here, the neural network was trained with soil  
214 temperature and soil moisture as independent variables, before ER was predicted across a range of  
215 conditions that cover the entire data set of flux tower measurements. GPP was derived as  $GPP = -$   
216  $NEE + ER$ , where  $-NEE = NEP$  (net ecosystem productivity). We converted the gap-filled latent  
217 heat flux ( $Wm^{-2}$ ) to evapotranspiration (ET; mm) and daily means of water use efficiency (WUE)  
218 were derived as  $WUE_{day} = \sum GPP / \sum ET$  ( $g\ C\ kg\ H_2O^{-1}$ ; Table 1). Further, we calculated the daily  
219 mean underlying  $WUE_{u\_day} = GPP \times VPD^{0.5} / ET$  ( $gC\ kPa^{-0.5}\ kgH_2O^{-1}$ ) to account for the non-linear  
220 effect of increasing VPD on LE (Zhou et al., 2015, 2014) and the daily mean intrinsic  $WUE_{i\_day} =$   
221  $GPP / Gc$  ( $gC\ mol^{-1}\ m^{-2}\ s^{-1}$ ) to quantify photosynthesis in relation to conductance (Beer et al., 2009;  
222 Lloyd et al., 2002; Schulze and Hall, 1982).

223 We calculated canopy conductance ( $Gc$ ;  $mol\ m^{-2}\ s^{-1}$ ) and potential evapotranspiration (PET; mm)  
224 following Monteith (1965), where we used site-specific meteorological observations from the flux  
225 tower measurements as input parameters, and identified the well-watered reference surface  
226 conductance as the average of the surface conductance when VPD was between 0.9 and 1.1 kPa  
227 and surface soil moisture exceeded the 75% quantile. To account for the energy imbalance when  
228 inverting the Penman-Monteith equation to calculate canopy conductance and PET (Knauer et al.,  
229 2018; Wilson et al., 2002), we set the available energy equal to the sum of the latent and sensible  
230 heat flux, which implicitly conserves the Bowen ratio (Wohlfahrt et al., 2009). Rainy periods were  
231 excluded from the analysis, and half-hourly data were resampled to hourly periods to reduce noise.

## 232 2.4 Climate variables and response functions

233 In addition to fluxes, we measured the following meteorological variables above the canopy:  
234 downwelling and upwelling, shortwave and thermal radiation (CNR1; Kipp and Zonen, Delft, The  
235 Netherlands), air temperature and relative humidity (Vaisala HMP155; Vaisala, Helsinki, Finland).  
236 Precipitation was recorded as half-hourly totals at 1 m below the canopy (TB6; Hydrological  
237 Services Pty Ltd, Warwick Farm, Australia), and we added an additional rain gauge of the same  
238 type above the canopy in July 2014. Soil moisture measurements were initially recorded only at  
239 10 and 40 cm depth close to the flux tower using time-domain measurement method to calculate  
240 soil volumetric water content (CS-616; Campbell Scientific Inc., Logan, UT, USA), and we  
241 extended these measurements by three additional sites adjacent to instrumented trees in November  
242 2013. Thereafter, each of the four sites contained a CS-650 at 10 cm depth (Campbell Scientific  
243 Inc., Logan, UT, USA) and three additional CS-616 at 40 cm, 65 cm and ca. 1 m depth (depending  
244 on soil texture), and measurements from the four pits were averaged for each depth. We used one-  
245 way ANOVAs followed by a Tukey test to assess significant differences in the response and key  
246 climate variables between the baseline, the driest and the hottest days and heatwave days. All data  
247 were analyzed in R version 3.5.1 (R Core Team, 2018) using the packages ‘dplyr’ and ‘reshape2’  
248 for manipulations, and ‘car’ for statistical analyses.

## 249 **3 Results**

### 250 3.1 Trade-offs between water loss and carbon gain

251 The daily sums of  $v_{\text{sap}}$ , ET, GPP and daily means of WUE differed significantly among the baseline  
252 days, the hottest and the driest days, and during the heatwave ( $P < 0.01$ ; Table 1). However, no  
253 variable was significantly different between the hottest days and the heatwave (Table 1),  
254 suggesting that the eucalypts did not respond differently to the longer heatwave compared with the

255 individual hot days. On the driest days,  $v_{\text{sap}}$  of both species remained comparable to the baseline,  
256 whereas  $v_{\text{sap}}$  increased by >45% during the hottest days and by >70% during the heatwave (Table  
257 1). Daily ET patterns resembled  $v_{\text{sap}}$  patterns, indicating that transpiration dominated the ET signal  
258 of this forest. Daily GPP was comparable between baseline days, the hottest days and during the  
259 heatwave, but was significantly reduced during the driest days (16% lower than the baseline days;  
260 Table 1). However, daily ER relative to the baseline increased by 36% during the driest days,  
261 doubled during the hottest days, and increased by 137% during the heatwave (resulting in  
262 significant differences among all groups with the exception of the hottest and heatwave days; Table  
263 1). This led to significant reductions in daily NEE relative to the baseline, which were in the order  
264 of 62% on the driest days, and 91% on the hottest days, and turned the forest from a moderate  
265 carbon sink to a carbon source (positive NEE) during the heatwave (Table 1).

266 Mean daytime canopy conductance relative to the baseline decreased significantly when soil  
267 moisture decreased (44% decrease in  $G_c$  during driest days with comparable mean daytime VPD;  
268 Table 1), and decreased further when VPD and temperatures increased during the hottest days and  
269 the heatwave (71% decrease in  $G_c$  despite comparable soil moisture to the baseline,  $P < 0.01$ ;  
270 Table 1). WUE estimations were most sensitive to the method of calculation on the hottest days  
271 and during the heatwave (up to 91% difference within the same group; Table 1). Using the total  
272  $\text{WUE}_{\text{day}}$ , the significant difference in GPP did not translate to significantly different  $\text{WUE}_{\text{day}}$   
273 between the baseline and the driest days, which remained at  $3 \text{ g C kg H}_2\text{O}^{-1}$  due to a comparable  
274 decrease in ET during the driest days. In contrast,  $\text{WUE}_{\text{day}}$  decreased by 34% ( $2.0 \pm 0.01 \text{ g C kg}$   
275  $\text{H}_2\text{O}^{-1}$ ) on the hottest days and by 42% ( $1.77 \pm 0.05 \text{ g C kg H}_2\text{O}^{-1}$ ) during the heatwave, which  
276 resulted in significantly lower WUE during hot days than on the driest and baseline days. However,  
277 the opposite trend occurred when accounting for the non-linear relationship between  $\text{GPP} \times \text{VPD}$

278 and ET at the ecosystem scale; that is, the underlying  $WUE_{u\_day}$  increased by 24% during the driest  
279 days ( $P < 0.01$ ; Table 1). Increasing WUE relative to baseline days was even more evident when  
280 based on the intrinsic  $WUE_{i\_day}$ , which increased by 30% during the driest days and by up to 125%  
281 during the hottest days and heatwave ( $P < 0.01$ ; Table 1), indicating that carbon assimilation  
282 (approximated as GPP) per unit stomatal conductance (approximated as  $G_c$ ) significantly  
283 increased during high temperatures and high VPD, a result that was not captured when using total  
284  $WUE_{day}$ .

285 **Table 1.** Overview of the key response and climate variables for baseline days, the hottest and the  
286 driest days, and during the heatwave. Values are mean daily sums and standard errors of water loss  
287 as sap velocity ( $v_{sap\_sum}$ ) for both species and as ecosystem-scale evapotranspiration ( $ET_{sum}$ ) and  
288 potential ET ( $PET_{EBC\_sum}$ ), as well as daily gross primary productivity ( $GPP_{sum}$ ), ecosystem  
289 respiration ( $ER_{sum}$ ), net ecosystem exchange ( $NEE_{sum}$ ), mean daytime canopy conductance  
290 ( $G_{cEBC\_day}$ ), water use efficiency ( $WUE_{day}$ ), underlying WUE ( $WUE_{u\_day} = GPP \times VPD^{0.5} / ET$ ) and  
291 intrinsic WUE ( $WUE_{i\_day} = GPP / G_c$ ), in addition to daily maximum vapor pressure deficit  
292 ( $VPD_{max}$ ) and temperature ( $T_{max}$ ), and daily mean soil water content ( $Swc_{mean}$ ) and incoming solar  
293 radiation ( $Fsd_{mean}$ ). Note that the subscript 'EBC' indicates that the available energy was set equal  
294 to the sum of the latent and sensible heat flux to account for the energy imbalance when inverting  
295 the Penman-Monteith combination equation to calculate canopy conductance and potential  
296 evapotranspiration. Different superscript letters indicate significant differences among the groups  
297 of days ( $P < 0.05$ , Tukey posthoc test).

	Baseline	Driest days	Hottest days	Heatwave
<b>V<sub>sap_sum</sub> <i>E. obliqua</i></b> (cm d <sup>-1</sup> )	597.6 ± 25.0 <sup>a</sup>	564.4 ± 23.3 <sup>a</sup>	867.9 ± 24.3 <sup>b</sup>	1017.1 ± 11.8 <sup>b</sup>
<b>V<sub>sap_sum</sub> <i>E. rubida</i></b> (cm d <sup>-1</sup> )	685.4 ± 32.6 <sup>a</sup>	717.6 ± 33.9 <sup>a</sup>	1083.7 ± 30.9 <sup>b</sup>	1281.5 ± 22.8 <sup>b</sup>
<b>ET<sub>sum</sub></b> (mm d <sup>-1</sup> )	2.88 ± 0.13 <sup>a</sup>	2.43 ± 0.15 <sup>a</sup>	4.12 ± 0.13 <sup>b</sup>	5.02 ± 0.16 <sup>b</sup>
<b>PET<sub>EBC_sum</sub></b> (mm d <sup>-1</sup> )	3.01 ± 0.20 <sup>a</sup>	3.91 ± 0.43 <sup>a</sup>	8.32 ± 0.38 <sup>b</sup>	9.62 ± 0.32 <sup>b</sup>
<b>GPP<sub>sum</sub></b> (g C d <sup>-1</sup> )	8.71 ± 0.28 <sup>b</sup>	7.3 ± 0.21 <sup>a</sup>	8.25 ± 0.22 <sup>ab</sup>	8.86 ± 0.32 <sup>ab</sup>
<b>ER<sub>sum</sub></b> (g C d <sup>-1</sup> )	4.07 ± 0.22 <sup>a</sup>	5.55 ± 0.36 <sup>b</sup>	7.85 ± 0.29 <sup>c</sup>	9.66 ± 0.31 <sup>c</sup>
<b>NEE<sub>sum</sub></b> (g C d <sup>-1</sup> )	-4.64 ± 0.34 <sup>a</sup>	-1.75 ± 0.48 <sup>b</sup>	-0.39 ± 0.37 <sup>b</sup>	0.79 ± 0.47 <sup>b</sup>
<b>G<sub>C<sub>EBC</sub>_day</sub></b> (mol m <sup>-2</sup> s <sup>-1</sup> )	0.48 ± 0.002 <sup>c</sup>	0.27 ± 0.004 <sup>b</sup>	0.14 ± 0.003 <sup>a</sup>	0.15 ± 0.008 <sup>a</sup>
<b>WUE<sub>day</sub></b> (gC kgH <sub>2</sub> O <sup>-1</sup> )	3.02 ± 0.02 <sup>b</sup>	3.01 ± 0.06 <sup>b</sup>	2.0 ± 0.01 <sup>a</sup>	1.77 ± 0.05 <sup>a</sup>
<b>WUE<sub>u_day</sub></b> (gC kPa <sup>-0.5</sup> kgH <sub>2</sub> O <sup>-1</sup> )	2.64 ± 0.02 <sup>a</sup>	3.27 ± 0.06 <sup>b</sup>	3.09 ± 0.03 <sup>ab</sup>	3.02 ± 0.08 <sup>ab</sup>
<b>WUE<sub>i_day</sub></b> (gC mol <sup>-1</sup> m <sup>2</sup> s <sup>-1</sup> )	2.11 ± 0.02 <sup>a</sup>	2.74 ± 0.07 <sup>a</sup>	4.51 ± 0.05 <sup>b</sup>	4.74 ± 0.07 <sup>b</sup>
<b>VPD<sub>max</sub></b> (kPa)	1.4 ± 0.1 <sup>a</sup>	1.93 ± 0.18 <sup>a</sup>	4.22 ± 0.15 <sup>b</sup>	4.56 ± 0.29 <sup>b</sup>
<b>T<sub>max</sub></b> (°C)	20.6 ± 0.7 <sup>a</sup>	24.2 ± 0.9 <sup>b</sup>	33.4 ± 0.4 <sup>c</sup>	35.3 ± 0.8 <sup>c</sup>
<b>SWC<sub>40cm_mean</sub></b> (m <sup>3</sup> m <sup>-3</sup> )	0.14 ± 0.002 <sup>b</sup>	0.1 ± 0.003 <sup>a</sup>	0.13 ± 0.003 <sup>ab</sup>	0.14 ± 0.001 <sup>b</sup>
<b>Fsd<sub>mean</sub></b> (W m <sup>-2</sup> )	304.0 ± 11.6 <sup>a</sup>	303.2 ± 13.4 <sup>a</sup>	351.2 ± 7.3 <sup>a</sup>	322.6 ± 21.1 <sup>a</sup>

299 3.2 The diurnal cycle in response to increasing VPD

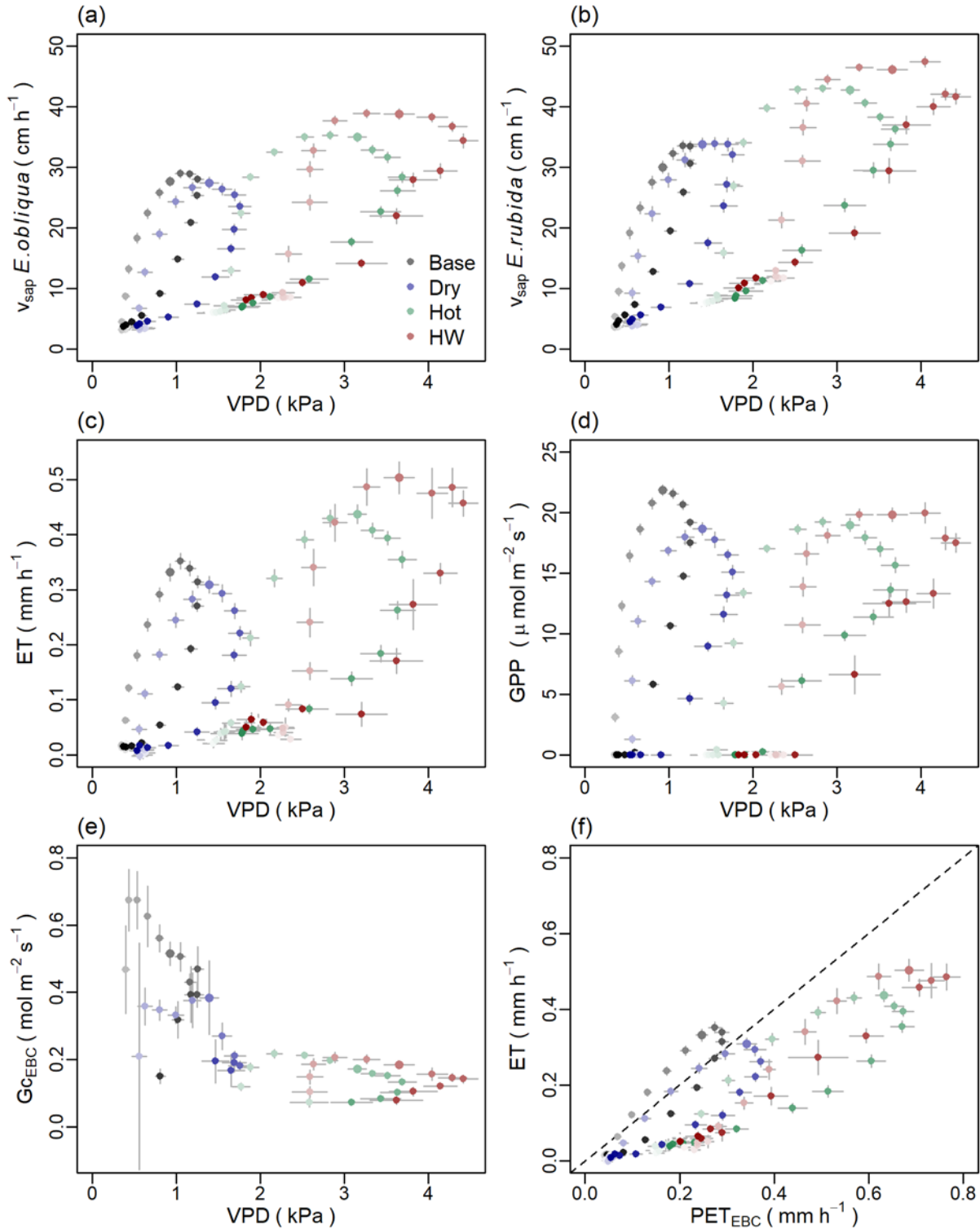
300 To further assess photosynthesis and water use during summer, we compared diurnal courses of  
301 Gc, GPP,  $v_{\text{sap}}$  and ET as a function of VPD (Fig. 2a-e). On the hottest days, maximum  $v_{\text{sap}}$   
302 increased significantly (by 22% for *E. obliqua* and 28% for *E. rubida*;  $P < 0.01$ ) compared with  
303 baseline days, and  $v_{\text{sap}}$  remained at these elevated levels while VPD was between 2.6 and 3.2 kPa.  
304 Thereafter, as VPD increased to 3.7 kPa in the mid-afternoon,  $v_{\text{sap}}$  decreased by 20% for *E. obliqua*  
305 and 16% for *E. rubida* (i.e. equal to the maximum  $v_{\text{sap}}$  on baseline days).  $v_{\text{sap}}$  rates peaked during  
306 the heatwave (39  $\text{cm h}^{-1}$  for *E. obliqua* and 47.4  $\text{cm h}^{-1}$  for *E. rubida*) and remained at these  
307 significantly elevated levels (34% for *E. obliqua* and 42% for *E. rubida* above their baseline  
308 maximum;  $P < 0.01$ ) until VPD exceeded 4.3 kPa. In contrast, on the driest days, increasing VPD  
309 decreased the peak  $v_{\text{sap}}$  of *E. obliqua* by 5%, while the peak  $v_{\text{sap}}$  for *E. rubida* remained comparable  
310 to the baseline maximum (Fig. 2a, b). Apart from this small deviation on the driest days, both  
311 species had a similar response to changes in VPD.

312 Consistent with  $v_{\text{sap}}$  dynamics, maximum ET at the ecosystem scale increased 24% on the hottest  
313 days and by 43% during the heatwave (Fig. 2c;  $P < 0.05$  for the heatwave). However, despite only  
314 minor or no reductions in maximum  $v_{\text{sap}}$  on the driest days, maximum ET decreased by 12% on  
315 the driest days relative to the summer baseline (Fig. 2c). As VPD increased in the afternoon, ET  
316 decreased between 9 to 28% until maximum VPD was reached during all conditions. Overall, ET  
317 dynamics were similar to  $v_{\text{sap}}$  dynamics, but more closely resembled the dynamics of *E. obliqua*  
318 than *E. rubida* due the decrease of ET with increasing VPD during the driest days.

319 In contrast to significant increases in peak  $v_{\text{sap}}$  and ET during the hottest days and the heatwave,  
320 the diurnal maximum of GPP declined with increasing VPD (Fig. 2d) and concurrently decreasing  
321 Gc (Fig. 2e) under both hot and dry conditions relative to the summer baseline (by 12% and 15%

322 on the hottest and driest days,  $P < 0.01$ ; and by 9% during the heatwave,  $P > 0.05$ ; Fig. 2d). Until  
323 maximum VPD was reached in the mid-afternoon, GPP decreased between 12 to 19% during all  
324 conditions (Fig. 2d). While reductions of peak GPP were comparable to reductions of peak ET  
325 during driest days (both decreased by 12%), the diurnal course of GPP and ET reversed during the  
326 heatwave: mid-day GPP was sustained within 9% of baseline days ( $P > 0.05$ ) at the cost of  
327 significantly increased peak ET (43% increase compared to the summer baseline,  $P < 0.05$ ).

328 Daytime canopy conductance varied considerably between the hottest, driest and baseline days  
329 (Fig. 2e): maximum  $G_c$  at baseline days was  $0.67 \text{ mol m}^{-2} \text{ s}^{-1}$ , which decreased by 43% and 68%  
330 on the driest and hottest days (to  $0.38$  and  $0.22 \text{ mol m}^{-2} \text{ s}^{-1}$ , respectively). Maximum  $G_c$  was  
331 comparable between hot days and the heatwave, despite a larger VPD range during the heatwave  
332 (Fig. 2e). However,  $G_c$  did not fully decline under any conditions, and the large reductions of  $G_c$   
333 on the driest, and especially on the hottest days and during the heatwave (Fig. 2e) only marginally  
334 affected GPP (Fig. 2d). Consequently, reductions in  $G_c$  primarily restricted excessive water loss  
335 during warm days with high atmospheric demand, which is supported by the ~50% reduction of  
336 ET compared to PET (Fig. 2f and Table 1) during the hottest days and during the heatwave. In  
337 addition, the close resemblance of diurnal ET and PET dynamics on the baseline and driest days  
338 indicate that the forest was only marginally water limited on these days (Fig. 2f).



339

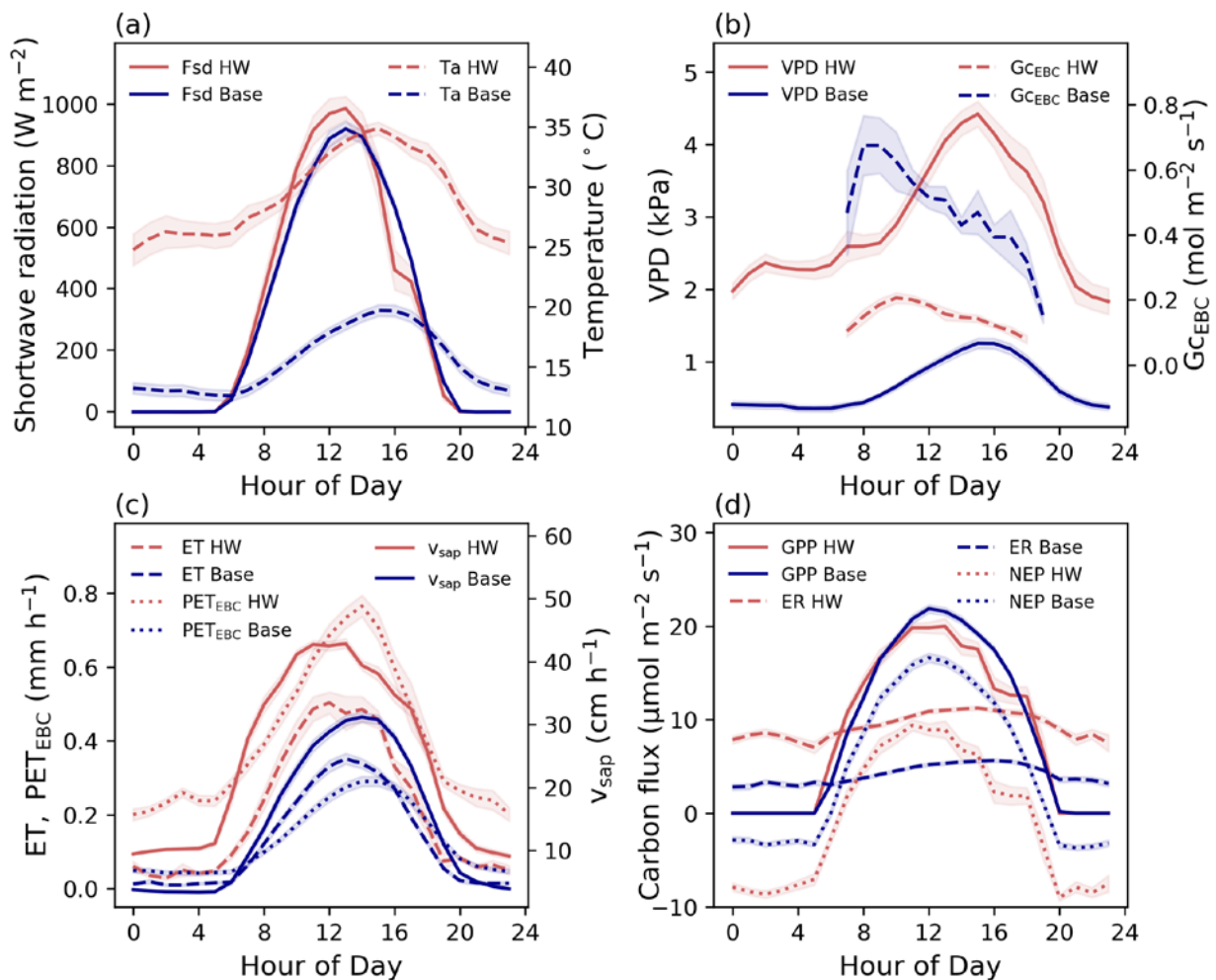
340 **Figure 2.** Diurnal patterns (means  $\pm$  standard error) of sap velocity ( $v_{\text{sap}}$ , cm h<sup>-1</sup>),  
 341 evapotranspiration (ET, mm h<sup>-1</sup>), gross primary productivity (GPP,  $\mu\text{mol m}^{-2} \text{s}^{-1}$ ), and daytime

342 canopy conductance ( $G_{\text{EBC}}$ ,  $\text{mol m}^{-2} \text{s}^{-1}$ ) in response to increasing vapor pressure deficit (VPD,  
343 kPa; panel a-e) and of ET against potential evapotranspiration ( $\text{PET}_{\text{EBC}}$ ,  $\text{mm h}^{-1}$ ; panel f) during  
344 the heatwave ('HW', red circles; 13-17 January 2014) on the hottest days ('Hot', green circles; air  
345 temperature  $> 30.7$  °C), driest days ('Dry', blue circles;  $\text{SWC} < 0.1 \text{ m}^3 \text{ m}^{-3}$ ) and baseline days  
346 ('Base', gray circles; January 2013, 2014 and 2015, excluding a hot period in January 2013, the  
347 January 2014 heatwave, and the hottest and driest days). Note that the subscript 'EBC' indicates  
348 that we set the available energy equal to the sum of the latent and sensible heat flux to account for  
349 the energy imbalance when inverting the Penman-Monteith combination equation to calculate  
350 canopy conductance and potential evapotranspiration. Symbols are colored according to the time  
351 of day (hourly time steps, shades darken with progression of the day) and the highlighted symbol  
352 indicates noon.

### 353 3.3 Carbon and water fluxes during a heat wave

354 The mean conditions during the five-day 2014 heatwave (13 to 17 January) compared with the  
355 local baseline for January 2013, 2014 and 2015 were characterized by similar soil moisture content  
356 ( $0.13\text{-}0.21 \text{ m}^3 \text{ m}^{-3}$  during the baseline and  $0.13\text{-}0.19 \text{ m}^3 \text{ m}^{-3}$  during the heatwave), but by 7% higher  
357 incoming radiation peak, markedly warmer minimum ( $11.5$  °C above baseline) and maximum  
358 temperatures ( $14.7$  °C above baseline), and ~four-fold higher atmospheric dryness (VPD), which  
359 peaked at  $\sim 4.6$  kPa in the early afternoon during the heatwave (Fig. 3a-b and Table 1). These  
360 increases in temperature and VPD resulted in a 37% increase in peak  $v_{\text{sap}}$  rates and a 70% increase  
361 in total daily water use compared to baseline days (averaged across both species; Fig. 3c and Table  
362 1). While peak PET increased three-fold during the heatwave, peak ET only increased by 43%  
363 compared to baseline days (Fig. 3c), leading to a 74% increase in total daily ET (from 2.88 mm on  
364 baseline days to 5.02 mm during the heat wave; Table 1). In contrast to increases in  $v_{\text{sap}}$  and ET,

365 the daily peaks and daily totals of GPP remained relatively unchanged during the heatwave,  
 366 indicating that baseline photosynthesis was maintained during the heatwave at the cost of  
 367 significantly increased transpiration (Table 1 and Fig. 3d). However, despite stable GPP, a  
 368 doubling of peak respiration rates ( $P < 0.05$ ) and a more than two-fold increase in daily ER ( $P < 0.01$ )  
 369 turned the forest from a moderate net carbon sink during baseline days ( $-4.64 \pm 0.34 \text{ g C d}^{-1}$ ) into  
 370 a net carbon source ( $0.79 \pm 0.47 \text{ g C d}^{-1}$ ) during the heatwave ( $P < 0.01$ ; Fig. 3d and Table 1).



371  
 372 **Figure 3.** The mean conditions during the heatwave (HW, 13-17 January 2014; red lines)  
 373 compared with the local baseline (Base, mean of January 2013-2015 without a hot period in 2013,

374 the 2014 heatwave and the hottest and driest days; blue lines). Abbreviations:  $F_{sd}$  = shortwave  
375 radiation ( $W m^{-2}$ ),  $T_a$  = air temperature ( $^{\circ}C$ ),  $VPD$  = vapor pressure deficit (kPa),  $G_{EBC\_day}$  = mean  
376 daytime canopy conductance ( $mol m^{-2} s^{-1}$ ),  $v_{sap}$  = sap velocity ( $cm h^{-1}$ , average of *E. obliqua* and  
377 *E. rubida*),  $ET$  = evapotranspiration ( $mm h^{-1}$ ),  $PET_{EBC}$  = potential evapotranspiration ( $mm h^{-1}$ ),  
378  $GPP$  = gross primary productivity ( $\mu mol m^{-2} s^{-1}$ ),  $NEP$  = net ecosystem productivity ( $\mu mol m^{-2} s^{-1}$ ),  
379  $ER$  = ecosystem respiration ( $\mu mol m^{-2} s^{-1}$ ). Note that shading represents standard error, and the  
380 subscript 'EBC' indicates that we set the available energy equal to the sum of the latent and  
381 sensible heat flux to account for the energy imbalance when calculating PET.

## 382 **4 Discussion**

### 383 4.1 Increased water use to sustain photosynthesis during high temperatures

384 Contrary to our first hypothesis, photosynthesis and water use within this dry-sclerophyll eucalypt  
385 forest were not always synchronous during summer, as we measured no significant change in  
386 photosynthesis in contrast to significantly increased water use in daily sums (Table 1), in response  
387 to increasing VPD (Fig. 2), and in diurnal patterns (Fig. 3) during the hottest days and during the  
388 5-day heatwave. On the hottest days and during the heatwave, photosynthesis was more-or-less  
389 sustained at the cost of >70% increased water loss relative to baseline days, which contrasted with  
390 concurrent decreases in both GPP (16%) and ET (16%) on the driest days. While hot or dry  
391 conditions resulted in decreased canopy conductance, this primarily restricted excessive water loss  
392 due to high atmospheric demand, and only marginally affected the GPP of this temperate eucalypt  
393 forest.

394 The ability to maintain photosynthesis across hot or dry conditions indicates a yield-focused  
395 growth strategy of the local eucalypt species, where carbon gain through photosynthesis is

396 prioritized over a conservative water use; this could partly explain the high annual carbon  
397 sequestration rates that have been reported for this forest in comparison with other temperate  
398 eucalypt forests (Beringer et al., 2016; Griebel et al., 2017; Hinko-Najera et al., 2017). Moreover,  
399 our findings demonstrate potential for temperate eucalypt forests growing in relatively mild, mesic  
400 conditions similar to our study site (e.g. at elevation or on cold sheltered sites with sufficient  
401 moisture supply) to maintain photosynthesis under future warmer climates, whereas eucalypt  
402 forests in less favorable growing conditions will likely increase stomatal adjustment to levels that  
403 adversely affect photosynthetic uptake (Drake et al., 2018; van Gorsel et al., 2016; Renchon et al.,  
404 2018). However, a doubling of ecosystem respiration turned the forest from a moderate net carbon  
405 sink into a net carbon source during the heatwave. Thus, while the photosynthesis of this eucalypt  
406 forest appears largely unaffected during warmer and drier conditions in the summer months, the  
407 over-proportional increase in ER resulted in a switch from a net sink to a source, highlighting that  
408 the net productivity can be adversely affected by isolated extreme events. Hence, with a projected  
409 increase in the number, duration and intensity of heat waves, the potential of temperate eucalypt  
410 forests to remain carbon sinks under future climates will largely depend on the response of  
411 ecosystem respiration to increasing temperatures rather than the ability to sustain photosynthesis  
412 during extreme heat.

413 The large increase in ET during the hottest days and the heatwave resulted in up to two-fold  
414 variations in total WUE in summer, with conflicting trends depending on the formulation of WUE  
415 (Table 1). While seasonal variation in WUE within the same ecosystem is typically linked to  
416 variations in canopy phenology (Huang et al., 2016; Jin et al., 2017), our observations were  
417 constrained to the summer season and pooled across three different summers with similar radiation  
418 input for all examined conditions (Fig. S1.), thereby minimizing phenological influences as well

419 as climatological variation. Yet, significant differences between the baseline and driest days in  
420 underlying WUE indicated that this metric was more sensitive to capturing physiological responses  
421 to drought stress than intrinsic WUE, possibly because  $WUE_{u\_day}$  reduces large parts of the diurnal  
422 and seasonal variation at the ecosystem scale within the same plant functional type (Zhou et al.,  
423 2015). In contrast,  $WUE_{i\_day}$  doubled during the hottest days and the heatwave, and accurately  
424 captured the significantly increased rate of photosynthesis per unit conductance. Despite different  
425 sensitivities of underlying and intrinsic WUE to either dry or hot conditions at our study site, none  
426 of these physiological responses were captured using the traditional formulation of WUE  
427 (GPP/ET), supporting that alternative formulations of WUE improved insights into the  
428 mechanisms regulating water loss and carbon uptake.

#### 429 4.2 Dependence on atmospheric demand

430 The influence of VPD on carbon and water fluxes has been well acknowledged (Beer et al., 2009;  
431 Eamus et al., 2013; Knauer et al., 2015; Novick et al., 2016; Renchon et al., 2018), and short- and  
432 long-term reductions in GPP and transpiration due to fluctuations in VPD and soil moisture have  
433 been recorded across a range of biomes even during non-drought years (Sulman et al., 2016).  
434 Further, a decrease in transpiration and photosynthesis due to stomatal regulation in response to  
435 increasing VPD is well established for eucalypts (Duursma et al., 2014; Mitchell et al., 2012;  
436 Pepper et al., 2008; Prior et al., 1997). While our study indicated that stomatal regulation of water  
437 loss can differ between exceptionally hot conditions and dry conditions, ecosystem-scale estimates  
438 of canopy conductance to infer stomatal activity are subject to large uncertainties as  $G_c$  is only  
439 inferred and not directly measured (Knauer et al., 2015; Wohlfahrt et al., 2009). While we  
440 attempted to minimize the contribution of non-transpirational water fluxes by removing rainy  
441 periods and by forcing energy balance closure (section 2.3), stomatal regulation might still be

442 confounded by anatomical properties of water transport; that is, the  $v_{\text{sap}}$  to VPD response can vary  
443 if the water absorption capacity at the root-soil interface becomes limiting or if the xylem anatomy  
444 restricts the water transport capacity from the roots to the canopy (Eamus & Prior, 2001; Sperry &  
445 Pockman, 1993; Tyree & Ewers, 1991). Still, ET was significantly reduced compared with PET on  
446 the hottest days and during the heatwave, providing clear indications of physiological regulations  
447 of water loss in response to increasing atmospheric demand in our forest, whereas the relative  
448 importance of stomatal regulations versus hydraulic restrictions on water transport remains  
449 unclear. Furthermore, the ability to maintain or even increase  $v_{\text{sap}}$  rates in all the conditions of our  
450 study suggests that the trees likely had access to soil water in deeper layers (section 4.3). Despite  
451 excluding rainy periods from our analyses, reduced peak rates and daily totals of ET on the driest  
452 days were not clearly due to decreases in  $v_{\text{sap}}$ , indicating a greater relative contribution of soil and  
453 canopy evaporation (or the lack thereof) to ecosystem-scale ET dynamics during dry conditions.  
454 Nevertheless, ET dynamics closely resembled  $v_{\text{sap}}$  dynamics of *E. obliqua*, confirming that stand-  
455 scale observations of ET were dominated by the transpiration dynamics of the dominating species  
456 (70% of stand basal area; Griebel 2016).

#### 457 4.3 Dependence on water availability

458 We can partially confirm our second hypothesis that evapotranspiration increases during a longer  
459 heatwave, however GPP remained comparable to baseline days and we did not measure a  
460 simultaneous sharp reduction in photosynthesis rates during the heatwave (as was measured for  
461 one-year old eucalypt saplings by Drake et al., 2018). This suggests that temperature stress may  
462 be ameliorated by water access at this comparatively mesic site. In addition to moderate moisture  
463 levels down to 1 m depth during the heatwave (ranging from 0.13 to 0.19  $\text{m}^3 \text{m}^{-3}$ ), sustained  $v_{\text{sap}}$   
464 even during the driest days suggests that the trees had access to deep water reserves, which were

465 likely recharged in the 2010/2011 LaNiña years when annual rainfall totals were ~200-400 mm  
466 above the long-term average. Eucalypts can have fast-growing roots that allow them to reach deep  
467 water resources quickly (e.g. 12 m depth in 2 years; Christina et al., 2017), and deep soil water  
468 access is known to be an important buffer in north Australia's open forests and savanna regions,  
469 where large amounts of water stored during the wet season can be accessed by trees during dry  
470 periods (Arndt et al., 2015; Eamus et al., 2015; Hutley et al., 2000; O'Grady et al., 1999). Even  
471 for temperate eucalypt forests in more complex terrain, access to water in deep soil layers has  
472 explained water losses that have exceeded annual precipitation inputs (Benyon & Doody, 2015;  
473 Mitchell et al., 2012). Hence, while access to deep soil water might represent an efficient  
474 adaptation of eucalypt trees to drought (Duursma et al., 2011; Markewitz et al., 2010; Nepstad et  
475 al., 2007; Yang et al., 2017), our study indicates that deep soil water access also plays an important  
476 role in explaining comparatively high carbon sequestration rates of temperate eucalypt forests.  
477 Furthermore, we found no evidence that the forest was exposed to severe heat or drought stress  
478 during our three observation years, which is supported by an absence of increased leaf shedding  
479 (Griebel et al., 2015) - a typical stress response for eucalypts (Granda et al., 2014; Pook, 1984;  
480 Renchon et al., 2018; Silva et al., 2004) - and by a sustained leaf area index whereby leaf loss was  
481 consistently balanced by growth of new leaves in our forest (Griebel et al., 2017). In addition,  
482 sustained photosynthetic rates during high temperatures indicate some buffer in the capacity of  
483 this forest type to maintain productivity under a warming climate; however, effects on productivity  
484 of very hot conditions combined with very dry conditions remain unclear, particularly if sustained  
485 dry conditions lead to a depletion in deep soil water reserves.

486 **5 Conclusions**

487 We present evidence that this temperate eucalypt forest was able to sustain photosynthesis at the  
488 cost of increased water loss during individual exceptionally hot days and during a longer heatwave,  
489 which contradicted our hypotheses of (i) concomitant reductions or increases in transpiration and  
490 photosynthesis, and (ii) notably decreasing photosynthesis with increasing transpiration during  
491 heatwaves. Increased or sustained transpiration rates during the hottest, driest and heatwave days  
492 indicated sufficient water availability to sustain photosynthesis rates at our study site, and  
493 consequently that neither individual hot or dry days, nor the heat wave coincided with water deficit  
494 and/or drought stress. This, in turn, indicated access of the roots to deeper water reserves. How  
495 sustainable such water reserves are, and how much these reserves will be depleted by prolonged  
496 heat waves or dry conditions remains unclear. Moreover, the switch from a net sink to a net source  
497 of carbon during the heatwave highlights potential limitations to similar, high elevation temperate  
498 eucalypt forests remaining carbon sinks under future climates, which will largely depend on the  
499 response of ecosystem respiration to increasing temperatures rather than their potential to maintain  
500 photosynthesis during hot or dry conditions.

501 **Acknowledgments**

502 We thank John Collopy and Julio Najera-Umana for assisting with the installation of the field  
503 equipment. This study was partly funded by TERN-OzFlux and TERN-SuperSites, the Australian  
504 Research Council (ARC) grants LE0882936 and DP120101735, and the Integrated Forest  
505 Ecosystem Research program supported by the Victorian Department of Environment Land, Water  
506 and Planning (DELWP). The flux tower data are available at the OzFlux portal  
507 (<http://data.ozflux.org.au>) and the tree water use data are available at Sapfluxnet

508 (<http://sapfluxnet.creaf.cat/app>). We appreciate substantive input from four anonymous reviewers  
509 which improved the quality of the manuscript.

## 510 **References**

511 Ameye, M., Wertin, T. M., Bauweraerts, I., McGuire, M. A., Teskey, R. O., & Steppe, K. (2012).  
512 The effect of induced heat waves on *Pinus taeda* and *Quercus rubra* seedlings in ambient and  
513 elevated CO<sub>2</sub> atmospheres. *New Phytologist*, *196*(2), 448–461.

514 Arndt, S. K., Sanders, G. J., Bristow, M., Hutley, L. B., Beringer, J., & Livesley, S. J. (2015).  
515 Vulnerability of native savanna trees and exotic *Khaya senegalensis* to seasonal drought. *Tree*  
516 *Physiology*, *35*(7), 783–791.

517 Ball, J. T., Woodrow, I. E., & Berry, J. A. (1987). A model predicting stomatal conductance and  
518 its contribution to the control of photosynthesis under different environmental conditions. In  
519 *Progress in photosynthesis research* (pp. 221–224). Springer.

520 Barr, A., Richardson, A., Hollinger, D., Papale, D., Arain, M., Black, T., et al. (2013). Use of  
521 change-point detection for friction–velocity threshold evaluation in eddy-covariance studies.  
522 *Agricultural and Forest Meteorology*, *171*, 31–45.

523 Beer, C., Ciais, P., Reichstein, M., Baldocchi, D., Law, B., Papale, D., Soussana, J., Ammann, C.,  
524 Buchmann, N., Frank, D., 2009. Temporal and among-site variability of inherent water use  
525 efficiency at the ecosystem level. *Global Biogeochemical Cycles* *23*.

526 Benyon, R. G., & Doody, T. M. (2015). Comparison of interception, forest floor evaporation and  
527 transpiration in *Pinus radiata* and *Eucalyptus globulus* plantations. *Hydrological Processes*, *29*(6),  
528 1173–1187.

529 Beringer, J., Hutley, L. B., McHugh, I., Arndt, S. K., Campbell, D., Cleugh, H. A., et al. (2016).  
530 An introduction to the Australian and New Zealand flux tower network - OzFlux. *Biogeosciences*,  
531 *13*(21), 5895–5916.

532 Breshears, D. D., Adams, H. D., Eamus, D., McDowell, N., Law, D. J., Will, R. E., et al. (2013).  
533 The critical amplifying role of increasing atmospheric moisture demand on tree mortality and  
534 associated regional die-off. *Frontiers in Plant Science*, *4*, 266.

535 Brouwers, N. C., Mercer, J., Lyons, T., Poot, P., Veneklaas, E., & Hardy, G. (2013). Climate and  
536 landscape drivers of tree decline in a Mediterranean ecoregion. *Ecology and Evolution*, *3*(1), 67–  
537 79.

538 Bureau of Meteorology (2013). *Special Climate Statement 43 – extreme heat in January 2013*.  
539 (BOM Publication No. SCS-43). Retrieved from  
540 <http://www.bom.gov.au/climate/current/statements/scs43e.pdf>

541 Bureau of Meteorology (2014). *Special Climate Statement 48 – one of southeast Australia’s most*  
542 *significant heatwaves*. (BOM Publication No. SCS-48). Retrieved from  
543 <http://www.bom.gov.au/climate/current/statements/scs48.pdf>

544 Bureau of Meteorology (2015). *Annual climate statement 2015*. Retrieved from  
545 <http://www.bom.gov.au/climate/current/annual/aus/2015/>.

546 Bureau of Meteorology (2016a). *Annual climate statement 2016*. Retrieved from  
547 <http://www.bom.gov.au/climate/current/annual/aus/2016/>.

548 Bureau of Meteorology (2016b). *Drought Statement - April rainfall reduces deficiencies in some*  
549 *areas*. Retrieved from <http://www.bom.gov.au/climate/drought/archive/20160505.shtml>.

550 Choat, B., Jansen, S., Brodribb, T. J., Cochard, H., Delzon, S., Bhaskar, R., et al. (2012). Global  
551 convergence in the vulnerability of forests to drought. *Nature*, 491(7426), 752.

552 Christina, M., Nouvellon, Y., Laclau, J. P., Stape, J. L., Bouillet, J. P., Lambais, G. R., & Maire,  
553 G. le. (2017). Importance of deep water uptake in tropical eucalypt forest. *Functional Ecology*,  
554 31(2), 509–519.

555 Cowan, I. (1978). Stomatal behaviour and environment. In *Advances in botanical research* (Vol.  
556 4, pp. 117–228). Elsevier.

557 De Kauwe, M.G., Medlyn, B.E., Pitman, A.J., Drake, J.E., Ukkola, A., Griebel, A. et al. (2019).  
558 Examining the evidence for decoupling between photosynthesis and transpiration during heat  
559 extremes. *Biogeosciences* 16, 903–916.

560 Drake, J. E., Tjoelker, M. G., Vårhammar, A., Medlyn, B. E., Reich, P. B., Leigh, A., et al. (2018).  
561 Trees tolerate an extreme heatwave via sustained transpirational cooling and increased leaf thermal  
562 tolerance. *Global Change Biology*. DOI: 10.1111/gcb.14037

563 Duursma, R. A., Barton, C. V. M., Eamus, D., Medlyn, B. E., Ellsworth, D. S., Forster, M. A., et  
564 al. (2011). Rooting depth explains CO<sub>2</sub> x drought interaction in *Eucalyptus saligna*. *Tree*  
565 *Physiology*, 31(9), 922–931.

566 Duursma, R. A., Barton, C. V. M., Lin, Y. S., Medlyn, B. E., Eamus, D., Tissue, D. T., et al.  
567 (2014). The peaked response of transpiration rate to vapour pressure deficit in field conditions can  
568 be explained by the temperature optimum of photosynthesis. *Agricultural and Forest Meteorology*,  
569 189, 2–10.

570 Eamus, D., & Prior, L. (2001). Ecophysiology of trees of seasonally dry tropics: Comparisons  
571 among phenologies. *Australian Journal of Botany*, 32, 113–197.

572 Eamus, D., Taylor, D. T., Macinnis-Ng, C. M., Shanahan, S., & De Silva, L. (2008). Comparing  
573 model predictions and experimental data for the response of stomatal conductance and guard cell  
574 turgor to manipulations of cuticular conductance, leaf-to-air vapour pressure difference and  
575 temperature: Feedback mechanisms are able to account for all observations. *Plant, Cell &*  
576 *Environment*, *31*(3), 269–277.

577 Eamus, D., Boulain, N., Cleverly, J., & Breshears, D. D. (2013). Global change-type drought-  
578 induced tree mortality: Vapor pressure deficit is more important than temperature per se in causing  
579 decline in tree health. *Ecology and Evolution*, *3*(8), 2711–2729.

580 Eamus, D., Zolfaghar, S., Villalobos-Vega, R., Cleverly, J., & Huete, A. (2015). Groundwater-  
581 dependent ecosystems: Recent insights from satellite and field-based studies. *Hydrology and Earth*  
582 *System Sciences*, *19*(10), 4229–4256.

583 Farquhar, G. D., & Sharkey, T. D. (1982). Stomatal conductance and photosynthesis. *Annual*  
584 *Review of Plant Physiology*, *33*(1), 317–345.

585 van Gorsel, E., Wolf, S., Cleverly, J., Isaac, P., Haverd, V., Ewenz, C., et al. (2016). Carbon uptake  
586 and water use in woodlands and forests in southern Australia during an extreme heat wave event  
587 in the “Angry summer” of 2012/2013. *Biogeosciences*, *13*(21), 5947–5964.

588 Granda, V., Delatorre, C., Cuesta, C., Centeno, M. L., Fernández, B., Rodríguez, A., & Feito, I.  
589 (2014). Physiological and biochemical responses to severe drought stress of nine *Eucalyptus*  
590 *globulus* clones: A multivariate approach. *Tree Physiology*, *34*(7), 778–786.

591 Griebel, A., Bennett, L. T., Culvenor, D. S., Newnham, G. J., & Arndt, S. K. (2015). Reliability  
592 and limitations of a novel terrestrial laser scanner for daily monitoring of forest canopy dynamics.  
593 *Remote Sensing of Environment*, *166*, 205–213.

594 Griebel, A. (2016). New approaches to investigate the seasonal growth dynamics in forests,  
595 (Doctoral dissertation). Retrieved from Minerva Access. (<http://hdl.handle.net/11343/112613>).  
596 Melbourne, Australia: The University of Melbourne.

597 Griebel, A., Bennett, L. T., Metzen, D., Cleverly, J., Burba, G., & Arndt, S. K. (2016). Effects of  
598 inhomogeneities within the flux footprint on the interpretation of seasonal, annual, and interannual  
599 ecosystem carbon exchange. *Agricultural and Forest Meteorology*, 221, 50-60.

600 Griebel, A., Bennett, L. T., & Arndt, S. K. (2017). Evergreen and ever growing - stem and canopy  
601 growth dynamics of a temperate eucalypt forest. *Forest Ecology and Management*, 389, 417–426.

602 Hinko-Najera, N., Isaac, P., Beringer, J., Gorsel, E. van, Ewenz, C., McHugh, I., et al. (2017). Net  
603 ecosystem carbon exchange of a dry temperate eucalypt forest. *Biogeosciences*, 14(16), 3781–  
604 3800.

605 Huang, M. T., Piao, S. L., Zeng, Z. Z., Peng, S. S., Ciais, P., Cheng, L., et al. (2016). Seasonal  
606 responses of terrestrial ecosystem water-use efficiency to climate change. *Global Change Biology*,  
607 22(6), 2165–2177.

608 Hughes, L., Cawsey, E., & Westoby, M. (1996). Climatic range sizes of Eucalyptus species in  
609 relation to future climate change. *Global Ecology and Biogeography Letters*, 23–29.

610 Hutley, L. B., O’Grady, A. P., & Eamus, D. (2000). Evapotranspiration from eucalypt open-forest  
611 Savanna of northern Australia. *Functional Ecology*, 14(2), 183–194.

612 Isaac, P., Cleverly, J., McHugh, I., Gorsel, E. van, Ewenz, C., & Beringer, J. (2017). OzFlux data:  
613 Network integration from collection to curation. *Biogeosciences*, 14(12), 2903–2928.

614 Jin, J., Zhan, W., Wang, Y., Gu, B., Wang, W., Jiang, H., et al. (2017). Water use efficiency in  
615 response to interannual variations in flux-based photosynthetic onset in temperate deciduous  
616 broadleaf forests. *Ecological Indicators*, 79(Supplement C), 122–127.

617 Jurskis, V. (2005). Eucalypt decline in Australia, and a general concept of tree decline and dieback.  
618 *Forest Ecology and Management*, 215(1–3), 1–20.

619 Knauer, J., Werner, C. & Zaehle, S. (2015). Evaluating stomatal models and their atmospheric  
620 drought response in a land surface scheme: A multibiome analysis. *Journal of Geophysical*  
621 *Research: Biogeosciences* 120, 1894–1911.

622 Knauer, J., Zaehle, S., Medlyn, B.E., Reichstein, M., Williams, C.A., Migliavacca, M. et al. (2018).  
623 Towards physiologically meaningful water-use efficiency estimates from eddy covariance data.  
624 *Global Change Biology* 24, 694–710.

625 Leuning, R. (1995). A critical appraisal of a combined stomatal-photosynthesis model for C3  
626 plants. *Plant, Cell & Environment*, 18(4), 339–355.

627 Markewitz, D., Devine, S., Davidson, E. A., Brando, P., & Nepstad, D. C. (2010). Soil moisture  
628 depletion under simulated drought in the Amazon: Impacts on deep root uptake. *New Phytologist*,  
629 187(3), 592–607.

630 Matusick, G., Ruthrof, K. X., Brouwers, N. C., Dell, B., & Hardy, G. S. J. (2013). Sudden forest  
631 canopy collapse corresponding with extreme drought and heat in a mediterranean-type eucalypt  
632 forest in southwestern Australia. *European Journal of Forest Research*, 132(3), 497–510.

633 McDowell, N., Pockman, W. T., Allen, C. D., Breshears, D. D., Cobb, N., Kolb, T., et al. (2008).  
634 Mechanisms of plant survival and mortality during drought: Why do some plants survive while  
635 others succumb to drought? *New Phytologist*, 178(4), 719–739.

636 McDowell, N. G. (2011). Mechanisms linking drought, hydraulics, carbon metabolism, and  
637 vegetation mortality. *Plant Physiology*, 155(3), 1051–1059.

638 Medlyn, B. E., Duursma, R. A., Eamus, D., Ellsworth, D. S., Prentice, I. C., Barton, C. V., et al.  
639 (2011). Reconciling the optimal and empirical approaches to modelling stomatal conductance.  
640 *Global Change Biology*, 17(6), 2134–2144.

641 Mitchell, P. J., Benyon, R. G., & Lane, P. N. J. (2012). Responses of evapotranspiration at different  
642 topographic positions and catchment water balance following a pronounced drought in a mixed  
643 species eucalypt forest, Australia. *Journal of Hydrology*, 440, 62–74.

644 Mitchell, P. J., O’Grady, A. P., Hayes, K. R., & Pinkard, E. A. (2014a). Exposure of trees to  
645 drought-induced die-off is defined by a common climatic threshold across different vegetation  
646 types. *Ecology and Evolution*, 4(7), 1088–1101.

647 Mitchell, P. J., O’Grady, A. P., Tissue, D. T., Worledge, D., & Pinkard, E. A. (2014b). Co-  
648 ordination of growth, gas exchange and hydraulics define the carbon safety margin in tree species  
649 with contrasting drought strategies. *Tree Physiology*, 34(5), 443–458.

650 Monteith, J. L. (1965). Evaporation and environment. *Symposium of the Society for Experimental*  
651 *Biology*, 19, 205–224.

652 Nepstad, D. C., Tohver, I. M., Ray, D., Moutinho, P., & Cardinot, G. (2007). Mortality of large  
653 trees and lianas following experimental drought in an Amazon forest. *Ecology*, 88(9), 2259–2269.

654 Novick, K. A., Ficklin, D. L., Stoy, P. C., Williams, C. A., Bohrer, G., Oishi, A. C., et al. (2016).  
655 The increasing importance of atmospheric demand for ecosystem water and carbon fluxes. *Nature*  
656 *Climate Change*.

657 O'Grady, A. P., Eamus, D., & Hutley, L. B. (1999). Transpiration increases during the dry season:  
658 Patterns of tree water use in eucalypt open-forests of northern Australia. *Tree Physiology*, *19*(9),  
659 591–597.

660 Pepper, D. A., McMurtrie, R. E., Medlyn, B. E., Keith, H., & Eamus, D. (2008). Mechanisms  
661 linking plant productivity and water status for a temperate eucalyptus forest flux site: Analysis  
662 over wet and dry years with a simple model. *Functional Plant Biology*, *35*(6), 493–508.

663 Pook, E. W. (1984). Canopy dynamics of *Eucalyptus-maculata* Hook .1. Distribution and  
664 dynamics of leaf populations. *Australian Journal of Botany*, *32*(4), 387–403.

665 Prior, L. D., Eamus, D., & Duff, G. A. (1997). Seasonal and diurnal patterns of carbon assimilation,  
666 stomatal conductance and leaf water potential in *Eucalyptus tetradonta* saplings in a wet-dry  
667 savanna in northern Australia. *Australian Journal of Botany*, *45*(2), 241–258.

668 R Core Team. (2018). *R: A language and environment for statistical computing*. Vienna, Austria:  
669 R Foundation for Statistical Computing. Retrieved from <https://www.R-project.org/>

670 Renchon, A. A., Griebel, A., Metzen, D., Williams, C. A., Medlyn, B., Duursma, R. A., et al.  
671 (2018). Upside-down fluxes Down Under: CO<sub>2</sub> net sink in winter and net source in summer in a  
672 temperate evergreen broadleaf forest. *Biogeosciences*, *15*(12), 3703-3716.

673 Schulze, E.-D. & Hall, A. (1982). Stomatal responses, water loss and CO<sub>2</sub> assimilation rates of  
674 plants in contrasting environments, in: *Physiological Plant Ecology I*. Springer, pp. 181–230.

675 Silva, F. C. e, Shvaleva, A., Maroco, J., Almeida, M., Chaves, M., & Pereira, J. (2004). Responses  
676 to water stress in two *Eucalyptus globulus* clones differing in drought tolerance. *Tree Physiology*,  
677 *24*(10), 1165–1172.

678 Smith, D. M., Larson, B. C., Kelty, M. J., & Ashton, P. M. S. (1997). *The practice of silviculture:*  
679 *Applied forest ecology*. Book, John Wiley; Sons, Inc.

680 Sperry, J., & Pockman, W. (1993). Limitation of transpiration by hydraulic conductance and xylem  
681 cavitation in *Betula occidentalis*. *Plant, Cell & Environment*, 16(3), 279–287.

682 Sulman, B. N., Roman, D. T., Yi, K., Wang, L. X., Phillips, R. P., & Novick, K. A. (2016). High  
683 atmospheric demand for water can limit forest carbon uptake and transpiration as severely as dry  
684 soil. *Geophysical Research Letters*, 43(18), 9686–9695.

685 Teuling, A.J., Seneviratne, S.I., Stöckli, R., Reichstein, M., Moors, E., Ciais, P. et al. (2010).  
686 Contrasting response of European forest and grassland energy exchange to heatwaves. *Nature*  
687 *Geoscience* 3, 722.

688 Thomas, D., & Eamus, D. (1999). The influence of predawn leaf water potential on stomatal  
689 responses to atmospheric water content at constant  $c_i$  and on stem hydraulic conductance and foliar  
690 abscisic acid concentrations. *Journal of Experimental Botany*, 50(331), 243–251.

691 Tuzet, A., Perrier, A., & Leuning, R. (2003). A coupled model of stomatal conductance,  
692 photosynthesis and transpiration. *Plant, Cell & Environment*, 26(7), 1097–1116.

693 Tyree, M. T., & Sperry, J. S. (1989). Vulnerability of xylem to cavitation and embolism. *Annual*  
694 *Review of Plant Biology*, 40(1), 19–36.

695 Tyree, M. T., & Ewers, F. W. (1991). The hydraulic architecture of trees and other woody plants.  
696 *New Phytologist*, 119(3), 345–360.

697 Urban, J., Ingwers, M. W., McGuire, M. A., & Teskey, R. O. (2017). Increase in leaf temperature  
698 opens stomata and decouples net photosynthesis from stomatal conductance in *Pinus taeda* and  
699 *Populus deltoides* x *nigra*. *Journal of Experimental Botany*, 68(7), 1757–1767.

700 Webb, E. K., Pearman, G. I., & Leuning, R. (1980). Correction of flux measurements for density  
701 effects due to heat and water-vapor transfer. *Quarterly Journal of the Royal Meteorological*  
702 *Society*, 106(447), 85–100.

703 Whitehead, D., & Beadle, C. L. (2004). Physiological regulation of productivity and water use in  
704 Eucalyptus: A review. *Forest Ecology and Management*, 193(1), 113–140.

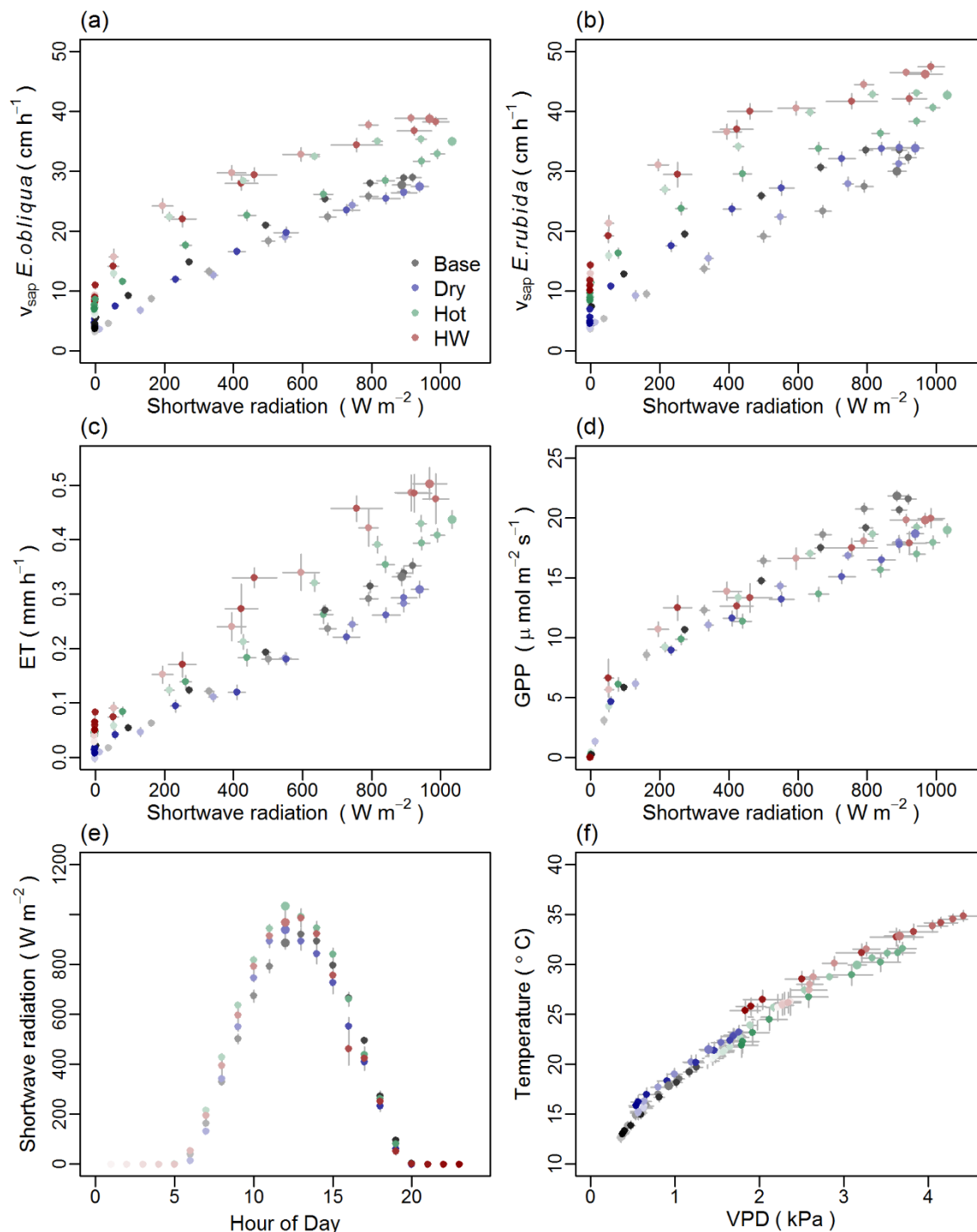
705 Wilson, K., Goldstein, A., Falge, E., Aubinet, M., Baldocchi, D., Berbigier, P. et al. (2002). Energy  
706 balance closure at Fluxnet sites. *Agricultural and Forest Meteorology* 113, 223–243.

707 Wohlfahrt, G., Haslwanter, A., Hortnagl, L., Jasoni, R.L., Fenstermaker, L.F., Arnone, 3., J. A. &  
708 Hammerle, A. (2009). On the consequences of the energy imbalance for calculating surface  
709 conductance to water vapour. *Agricultural and Forest Meteorology* 149, 1556–1559.

710 Yang, F. T., Feng, Z. M., Wang, H. M., Dai, X. Q., & Fu, X. L. (2017). Deep soil water extraction  
711 helps to drought avoidance but shallow soil water uptake during dry season controls the inter-  
712 annual variation in tree growth in four subtropical plantations. *Agricultural and Forest*  
713 *Meteorology*, 234, 106–114

714 Zhou, S., Yu, B., Huang, Y., & Wang, G. (2014). The effect of vapor pressure deficit on water use  
715 efficiency at the subdaily time scale. *Geophysical Research Letters* 41, 5005–5013.

716 Zhou, S., Yu, B., Huang, Y. & Wang, G. (2015). Daily underlying water use efficiency for  
717 Ameriflux sites. *Journal of Geophysical Research: Biogeosciences* 120, 887–902.



719  
 720 **Figure S1.** Diurnal patterns (means  $\pm$  standard error) of sap velocity ( $v_{sap}$ ,  $cm h^{-1}$ ),  
 721 evapotranspiration (ET,  $mm h^{-1}$ ), gross primary productivity (GPP,  $\mu mol m^{-2} s^{-1}$ ) against solar

722 radiation (Shortwave radiation,  $\text{W m}^{-2}$ ; panel a-d), as well as the diurnal course of shortwave  
723 radiation (panel e) and of VPD against air temperature ( $^{\circ}\text{C}$ ; panel f) during the heatwave ('HW',  
724 red circles; 13-17 January 2014) on the hottest days ('Hot', green circles; air temperature  $> 30.7$   
725  $^{\circ}\text{C}$ ), driest days ('Dry', blue circles;  $\text{SWC} < 0.1 \text{ m}^3 \text{ m}^{-3}$ ) and baseline days ('Base', gray circles;  
726 January 2013, 2014 and 2015, excluding a hot period in January 2013, the January 2014 heatwave,  
727 and the hottest and driest days). Symbols are colored according to the time of day (hourly time  
728 steps, shades darken with progression of the day) and the highlighted symbol indicates noon.